HYDROGELS

Cuticular pad–inspired selective frequency damper for nearly dynamic noise–free bioelectronics

Byeonghak Park[1], Joo Hwan Shin[1], Jehyung Ok[1], Subin Park[1], Woojin Jung[1], Chanho Jeong[2], Seunghwan Choy[1], Young Jin Jo[1], Tae-il Kim[1,2,3]*

Bioelectronics needs to continuously monitor mechanical and electrophysiological signals for patients. However, the signals always include artifacts by patients' unexpected movement (such as walking and respiration under approximately 30 hertz). The current method to remove them is a signal process that uses a bandpass filter, which may cause signal loss. We present an unconventional bandpass filter material—viscoelastic gelatin-chitosan hydrogel damper, inspired by the viscoelastic cuticular pad in a spider—to remove dynamic mechanical noise artifacts selectively. The hydrogel exhibits frequency-dependent phase transition that results in a rubbery state that damps low-frequency noise and a glassy state that transmits the desired high-frequency signals. It serves as an adaptable passfilter that enables the acquisition of high-quality signals from patients while minimizing signal process for advanced bioelectronics.

Advanced bioelectronics such as wearable (*1*, *2*) and implantable (*3*, *4*) devices are considered highly promising for the continuous detection and measurement of human physiological signals (*5*, *6*). Although recent accomplishments involving the integration of soft and flexible materials with ultrathin electronics (*7*, *8*) have enabled continuous monitoring (*9*, *10*) and multifunctionality (multimodal sensing and stimulation) (*11*–*13*), such applications (for example, in patient care) are generally limited by signal artifacts that arise from dynamic noise (usually under 30 Hz) (*14*, *15*). These signal artifacts include noise arising from patient movements, such as breathing, walking, tapping, and running. To selectively remove the dynamic noise embedded in these biosignals, processing techniques such as bandpass filtering are used (*14*). However, that can cause loss of information (*15*) and hardly change the band on demand (table S1). And wirelessly transfer of their whole signals, including noises in miniaturized wearable electronics, suffer from signal delay in the signal processing. Although damping materials that have shock-absorbing properties could be useful, they need to be designed to damp the wide or selective ranges of frequency of biophysiology.

Spiders can use their webs to monitor minute vibration signals generated by their prey, enemies, and mates, even in noisy (windy or rainy) conditions, which usually correspond to low-frequency (~30 Hz) vibrations (Fig. 1A) (*16*). Spiders can separate target vibration signals from mechanical noise using a selective vibration frequency damping organ in the form of a cuticular pad located under the vibration receptor (fig. S1) (*16*, *17*). The cuticular pad has viscoelastic properties that result from viscous bonds such as hydrogen bonds between chitin and protein chains, and the pad material phase changes from a rubbery to a glassy state above an applied frequency of near 30 Hz (Fig. 1B) (*17*). This phase transition allows the pad to selectively transmit target vibration signals (higher than 30 Hz) and filter low-frequency noise (lower than 30 Hz).

We fabricated a chitosan and gelatin interpenetrating hydrogel damper (fig. S2 and movie S1). The dynamic mechanical properties of the hydrogel are similar to those of the spider's cuticular pad, with modulus increasing with frequency (Fig. 1C). The material enables viscous damping below the transition frequency. Above the transition frequency, the tan δ value decreases while the modulus increases with frequency, so that vibrations elastically transmit. Attributed to its low-frequency damping, the hydrogel can be used in eliminating dynamic noises under 30 Hz (Fig. 1D and fig. S3). The key mechanism we hypothesize for selective damping is based on the relaxation time of the viscoelastic material, determining the material's transition frequency (Fig. 1E). The ratio of the relaxation time to the deformation time (observation time) is defined as *De*, which characterizes the viscoelasticity of the material. When a vibration stimulus reaches the hydrogel damper, the weak bonds responsible for the viscosity partially break and absorb the vibration energy, resulting in a rubbery state. If the relaxation time is less than the vibration period ($De < 1$; viscous) and the mechanical stress is quickly recovered before the next period of the vibration, then the vibration is continuously absorbed. As the frequency increases up to the transition point ($De = 1$), shear thickening occurs, and the viscosity increases because of the friction between the chains with remaining viscosity-related bonds, and the damping is maximized. However, if the relaxation time is longer than the vibration period ($De > 1$; elastic), meaning that the stress does not recover before the next period of the vibration, then the absorption fails, the chains rearrange, and the vibration transmits.

To investigate the selective damping property of the hydrogel damper composed of semi-interpenetrating hydrogels with gelatin and chitosan, we implemented dynamic mechanical analysis through the frequency sweep with chitosan, gelatin, and gelatin-chitosan hydrogel (Fig. 1F). The chitosan maintains a high tan δ value because of its viscous bonds between its chains in overall frequency, whereas gelatin has an apparent phase transition (*18*, *19*). We hypothesize that the external vibration stimulus dissociates the viscous bonds, such as hydrogen bonds, of the polymer matrix from dominantly chitosan hydrogel, dissociates hydrophobic interactions from dominantly gelatin hydrogel, and rearranges chitosan and gelatin chains in the manner of the stimulus (fig. S2) (*20*). Mixtures of gelatin and chitosan exhibit both high damping and phase transition, so that the selective frequency damping can be realized. The mechanical compression test shows decreasing hysteresis on the frequency (fig. S4) by shear-thickening damping properties, and the damping mechanism predominantly comes from the break and recovery of the viscous weak bonds (fig. S5). The highpass filter characteristics can be shown with 14.18 dB/decade at 27°C and 59.69 dB/decade at 45°C in a Bode plot (fig. S6 and table S2).

These selective frequency-damping properties can be used in bioelectronics. Dynamic noise from motion artifacts is found over a wide frequency range (Fig. 1G), from 0.01 to nearly 15 Hz, including even involuntary mechanical signals, such as respiration (0.1 to 1 Hz), heartbeat (0.3 to near 4 Hz), and gait motion (1 to 15 Hz) signals (*21*–*23*). Integration with the hydrogel material on conventional electrodes can be compatible to detect electrophysiological signals such as electroencephalogram (EEG) and electrocardiogram (ECG) signals (Fig. 1H). The hydrogel damper electrode targets the elimination of low-frequency mechanical noise while transmitting electrical biophysiological signals through an electrical pathway. To apply our selective damping material to the detection of distinct mechanical biophysiological signals, we designed a prototype device that consists of a 2-mm-thick hydrogel coated on a mechanosensor. We demonstrate a nanoscale crack-based mechanosensor inspired by a spider's vibration-sensing slit organ, with a Bluetooth module for wireless data acquisition and a closed-loop compensation system for temperature variation

[1]School of Chemical Engineering, Sungkyunkwan University (SKKU), Suwon 16419, Republic of Korea. [2]Department of Biomedical Engineering, SKKU, Suwon 16419, Republic of Korea. [3]Biomedical Institute for Convergence at SKKU (BICS), SKKU, Suwon 16419, Republic of Korea.
*Corresponding author. Email: taeilkim@skku.edu

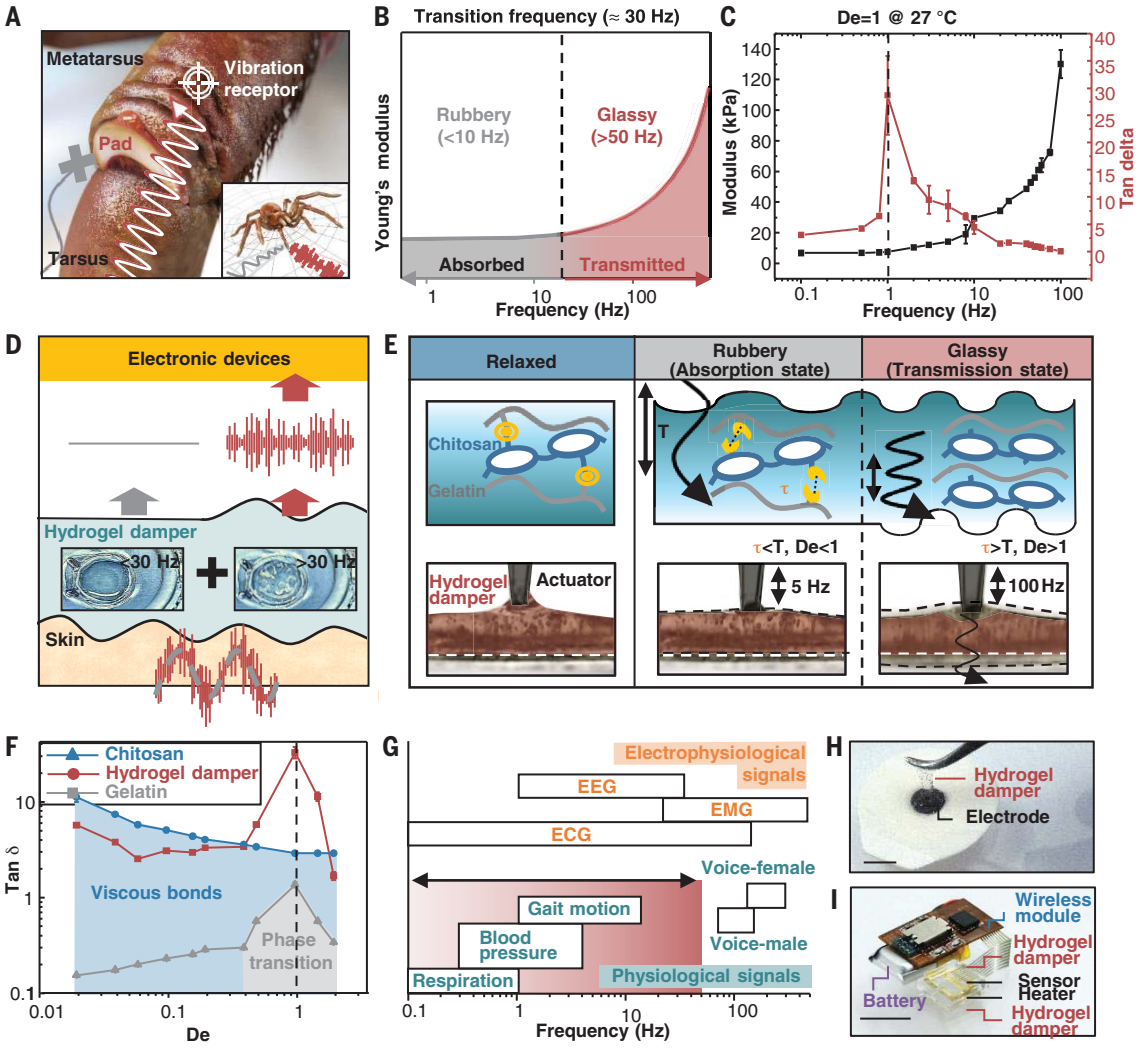

Fig. 1. Selective noise damping in a spider's cuticular pad and the bioinspired gelatin-chitosan hydrogel damper for selective frequency-dependent damping. (**A**) Schematic illustrations of selective low-frequency damping of superposed high-frequency target signals (>30 Hz) at the viscoelastic cuticular pad between the tarsus and metatarsus. The selectively transmitted target signals reach the lyriform slit organs (vibration receptor). (**B**) Viscoelastic properties of the spider's pad, which depend on the applied frequency of vibration (*28*). The mechanical properties of the damping pad include a rubber-glass transition under an ~30-Hz vibration. (**C**) Dynamic mechanical storage modulus and tan δ of the gelatin-chitosan hydrogel versus frequency (n = 3 samples, mean ± SD). (**D**) Schematic illustration of selective biophysiological signal detection through the hydrogel damper from skin and the surroundings. At high frequency, the vibration starts to transmit through the hydrogel damper surface, with the plate vibration patterns visualized on the surface. (**E**) Selective damping mechanism in the hydrogel damper related to the relaxation time. The transition between absorption and transmission is determined by the *De* of the hydrogel damper. The hydrogel damper on 1.5 μm polyethylene terephthalate (PET) (white dotted lines) fluctuates under a 100-Hz vibration, transmitting the vibrations *De* > 1. (**F**) Dynamic tan δ curves of chitosan, gelatin, and the gelatin-chitosan hydrogel below and above *De* = 1. (**G**) Representative frequency ranges of human mechanical (blue) and electrophysiological (orange) biosignals and mechanical damping ranges of the hydrogel damper (red) in the 27° to 45°C temperature range (*21*–*23*). (**H** and **I**) Example of bioelectronics by the hydrogel damper electrode for measuring electrophysiological signals (H) with mechanical noise and (I) incorporated with the hydrogel damper for selective mechanical target signal detection by a crack-based strain sensor connected to a Bluetooth module. Scale bars, (H) 1 cm; (I) 8 mm.

by use of a heater and thermocouple (Fig. 1I and fig. S7).

Engineering the relaxation time of the hydrogel damper can shift the damping curve and transmitted frequencies according to users' demand. When the polymeric chains have a higher diffusion rate, they have more chances to recover their stress, leading to fast relaxation time under the given mechanical stimulus (Fig. 2A). The relaxation time is determined by the temperature and molecular weight of gelatin, which affects the diffusion rate of the chains, as confirmed with the Rouse model in tube theories (Fig. 2B and figs. S2 and S8) (*24*). The water content can be one of the factors for the viscoelasticity, but for stability, the concentration was fixed at 6 wt % on the basis of the optimization (fig. S9). The relaxation time changes from 1.11 to less than 0.0193 s (Fig. 2B). Drop-ball tests with a 3.2-mm-diameter stainless steel ball on the hydrogel substrates represent elastic transmission and reflection of mechanical energies at 19°C, where the *De* number is ≫1, whereas the damping of mechanical energies occurs after the temperature is increased to 45°C, where *De* is ≪1 (Fig. 2C and movie S2). The viscoelastic properties can be controlled by tuning the temperature, as exemplified by our ability to shift the damping frequency from 0.89 to 51.8 Hz by changing the temperature from 27° to 45°C (Fig. 2D); in this way, the damping frequency can be tuned according to the user requirements (fig. S10).

Transmitted vibration amplitudes through the hydrogel damper (Fig. 2E, red) and polydimethylsiloxane (PDMS) reference (Fig. 2E, gray) at 27° and 45°C with 10 s of vibrations (5, 25, and 100 Hz) and a temperature sweep (from 18° to 45°C) at three applied vibration frequencies (5, 25, and 100 Hz) (Fig. 2F) implies that selective frequency damping and shifting of the frequencies is feasible (fig. S8). For the

25-Hz vibration, there is a marked decrease in transmission with the temperature that reflects the temperature-induced transition-point shift compared with the continuous-absorption 5 Hz and transmission 100 Hz (Fig. 2F). Even with multiple superposed vibrations, selective damping by the hydrogel damper at 5 Hz occurs at 27°C (Fig. 2G), whereas raising the temperature to 45°C enables the damping frequency to be increased to 51.8 Hz. By contrast, the PDMS elastomer transmits vibrations regardless of frequency and temperature because of its elastic properties. Morlet wavelet transform images demonstrate the selective damping properties and shifts in the hydrogel damper

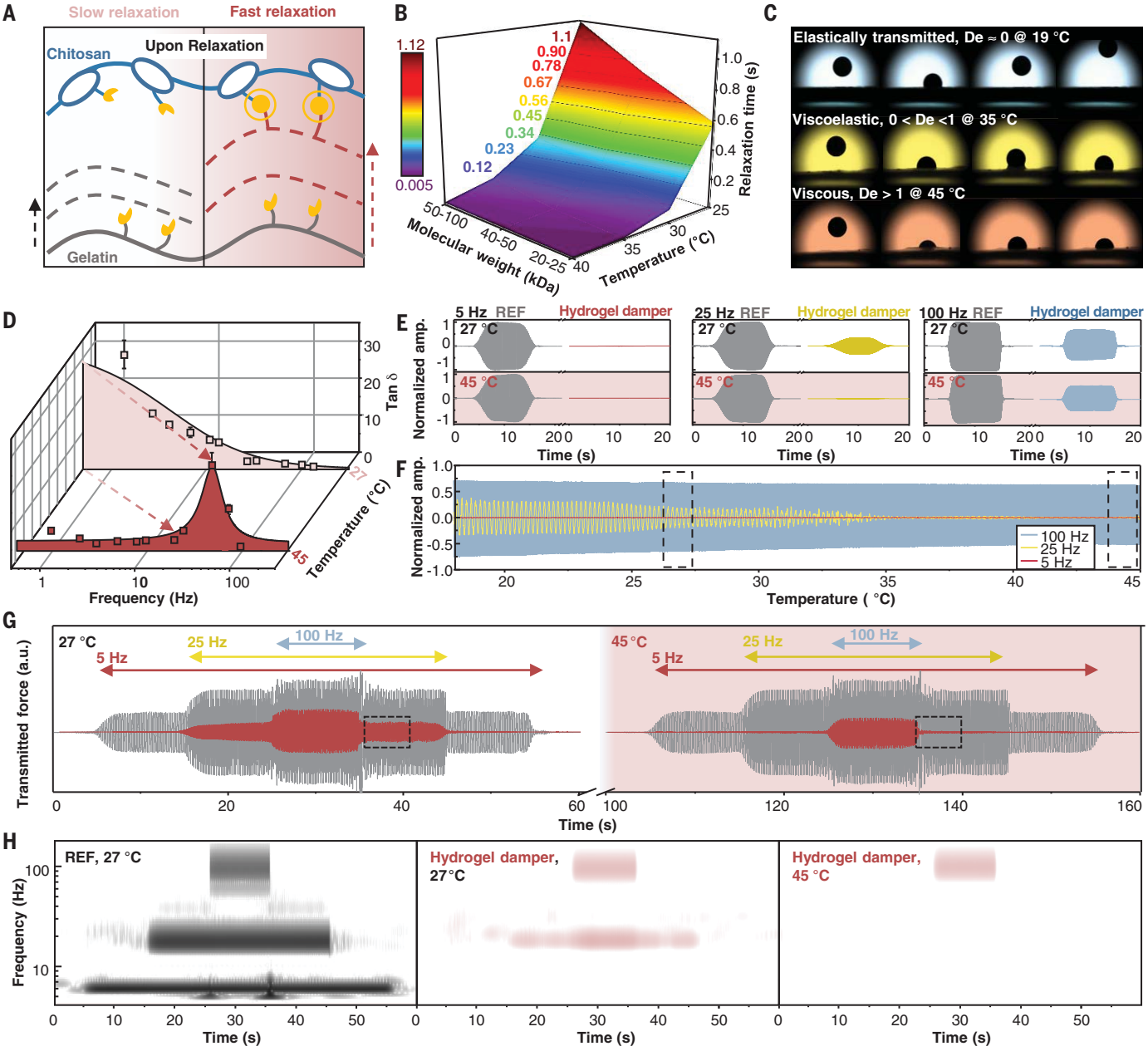

Fig. 2. Shifting the damping region by tuning the relaxation time, which corresponds to the transition frequency. (**A**) Schematic illustration of chain relaxation after a vibration stimulus in relatively (left) low-temperature and (right) high-temperature atmospheres. A higher temperature accelerates the relaxation. (**B**) Temperature and molecular weight dependency of the relaxation time and transition frequency of the hydrogel damper. The transition frequency is the reciprocal of the observed relaxation time when *De* = 1. (**C**) Viscoelastic transmission and damping at different temperatures (19°, 35°, and 45°C), with *De* verified by dropping metal balls on the hydrogel layer. (**D**) Shifting of the hydrogel damper transition frequency from 0.89 Hz at 27°C to 51.8 Hz at 45°C. (**E**) Measured real-time waveforms of vibrations in reference (gray) and the hydrogel damper samples with 5- (red), 25- (yellow), and 100-Hz (sky blue) frequencies individually applied at ambient temperature (27°C, top) and in a 45°C atmosphere (bottom). (**F**) Normalized waveforms of transmitted vibrations with 5 (red), 25 (yellow), and 100 Hz (sky blue) frequencies individually applied upon a temperature change from 18° to 45°C. The dotted box indicates the waveforms at ambient temperature (27°C) and 45°C. (**G**) Measured real-time waveform of vibrations in a reference (gray) and the hydrogel damper (red) with superposed 5-, 25-, and 100-Hz multiple-vibration frequencies applied at (left) ambient temperature (27°C) and (right) in a 45°C atmosphere. (**H**) Morlet wavelet transform of each vibration transmitted through a reference at 27°C and the hydrogel damper at 27°C and 45°C.

damping curve between 27° and 45°C; the damping by the reference is shown for comparison (Fig. 2H).

We compared the damping properties with commercially available polymeric dampers—D3O (*25*), Alphagel (Theta 7) (*26*), a silicone-based elastomer (PDMS), and a shear-thickening cornstarch suspension—that are viscoelastic shear thickening materials for shock absorption. When each damper's absorbed energy per volume is measured at various frequencies to investigate energy absorption capability (Fig. 3A), the peak damping energies in the hydrogel damper case, at both 27° and 45°C, are at least 6.7 times higher (113.04 mJ/mm^3 at 27°C and 108.62 mJ/mm^3 at 45°C) than the next best-performing damping material. Even though the damping curve can be shifted by tuning the temperature, the amount of absorbed energy shows the only minimal change. Attributed to the apparent phase transition of the hydrogel damper, the relaxation time changes, and transition frequencies eventually show dramatic changes under the temperature (Fig. 3B). The absorbed energy comparison of the hydrogel damper shows superior selectivity between the noise and target signals (338.73 at 27°C and 282.39 at 45°C), which is more than 20 times those of the other damping materials (Fig. 3C). The hydrogel damper also exhibits a damping factor that is more than 3.35 times larger (22 mJ·s/m^3 at 27°C and 5.7 mJ·s/m^3 at 45°C) than those of the other damping materials (Fig. 3D). Thus, in the case of the hydrogel damper, the damping bandwidths are narrow (80.59 Hz at 27°C and 169.3 Hz at 45°C), whereas other dampers show broad bandwidths (Fig. 3E). Among a broader range of material types in an Ashby plot, the hydrogel damper is located close to conventional hydrogels, near the kilopascal range (Fig. 3F). The hydrogel damper surpasses the tan δ over the elastomers and polymers with the ranges of the kilopascal modulus ranges.

We applied the hydrogel damper into bioelectronics for continuous biosignal detection without signal processing. The amount of water passivated in the hydrogel damper that is laminated on the different skin spots (chest, neck, wrist, and forehead) does not change significantly (figs. S9 and S11). First, to separate target mechanical signals from low-frequency dynamic noise, we assembled the hydrogel damper with an ultrasensitive crack-based strain sensor (Fig. 1I and fig. S12) (*27*, *28*). One example would be to acquire speech

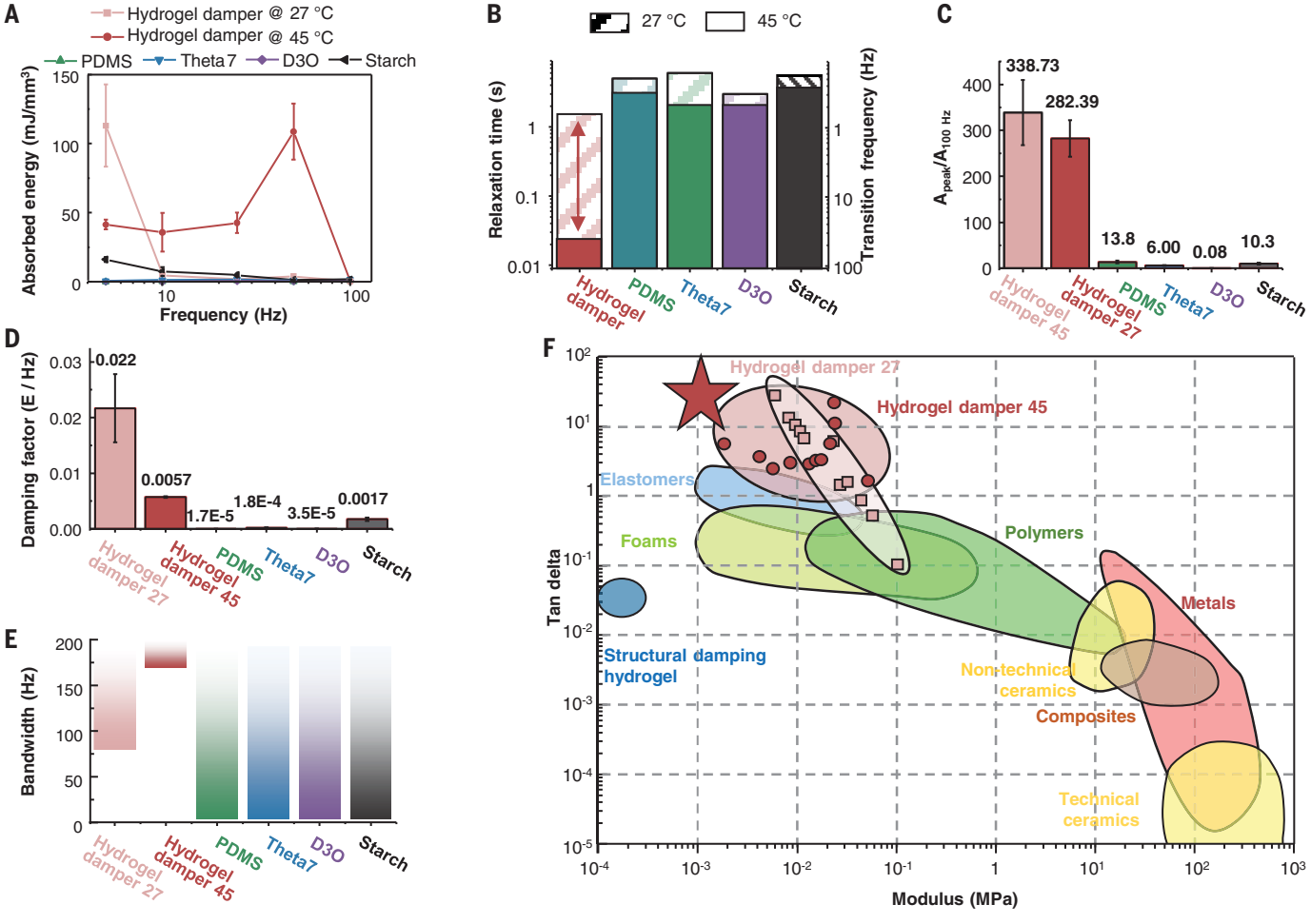

Fig. 3. Damping properties of the gelatin-chitosan hydrogel damper compared with other damping materials. (**A**) Absorbed energy per volume for the hydrogel damper at 27°C (pink) and 45°C (red) and for representative damping materials [PDMS (green), Theta 7 (blue), D3O (purple), and 55% cornstarch solution (black)] (n = 5 samples, mean ± SD). (**B**) Relaxation time changes and transition frequency changes with temperature (27° and 45°C) for the hydrogel damper and other damping materials. (**C**) Amplitude difference between peak frequency and 100 Hz for the hydrogel damper at 27° and 45°C and other damping materials. (n = 5 samples, mean ± SD). (**D**) Damping factors for bandpass filtering by the hydrogel damper and other damping materials. (n = 5 samples, mean ± SD). (**E**) Bandwidth comparison of hydrogel damper at 27°C and 45°C and other damping materials. (**F**) Energy damping diagram of the hydrogel damper and other materials (*30*).

information without dynamic noises deployed on the neck (Fig. 4A). The frequency of neck vibration during speech is usually at least 100 Hz, whereas physical noise arises from motions such as swallowing and skin tension due to movement, which usually has frequencies under 30 Hz (Fig. 4B) (*22*, *23*). A male volunteer spoke "Viva la vida" after attaching the integrated sensor to his neck (Fig. 4C, yellow arrows), and then the volunteer performed a swallowing motion to create dynamic noise (Fig. 4C, black arrows). Even if the sensor has low-frequency dynamic noise induced by the tension of the skin or movement, it contributes over a wide frequency range because the noise can

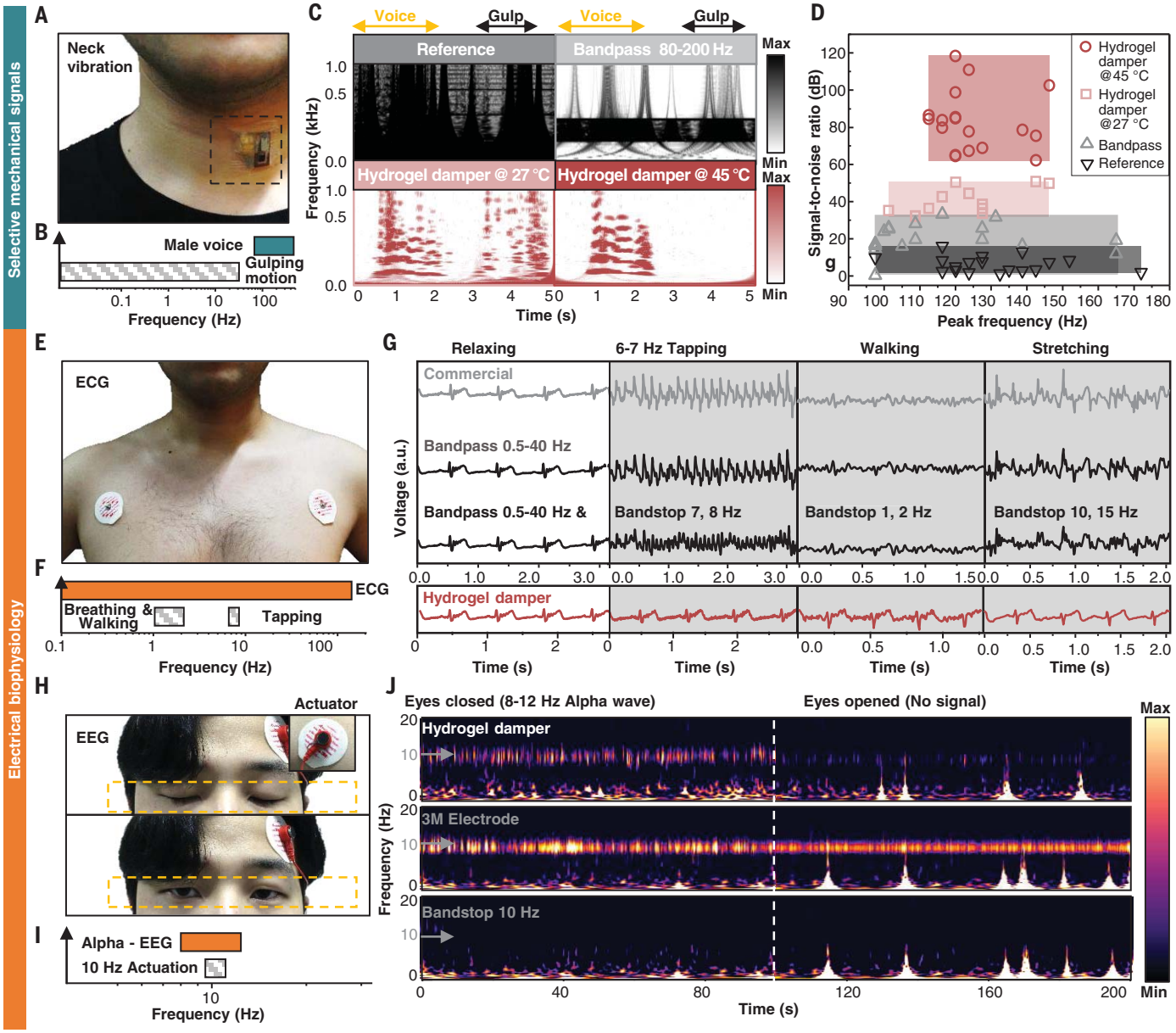

Fig. 4. Demonstration of dynamic noise-damping by using the hydrogel damper for high SNR detection of biophysiological signals. (**A**) Demonstration of human speech recording based on neck vibration by using wireless mechanical sensing with the hydrogel damper and PDMS as a reference. (**B**) Frequency ranges of a male voice and a swallowing motion (~20 Hz). (**C**) Comparisons of auditory spectrograms measured (top) without and (bottom) with the hydrogel damper during the pronunciation of "Viva la vida" and the swallowing motion. Black and gray spectra show reference and bandpass-filtered signals. The acoustic neck vibrations were detected with a reference crack-based sensor on a piece of PDMS and the hydrogel damper at 27°C and 40°C. For comparison, the signals from the reference crack-based sensor were treated with bandpass filtering from 80 to 200 Hz. (**D**) SNR comparison for the detected voice at each peak frequency for the hydrogel damper and reference (PDMS) (n = 18 samples). (**E**) Potential application in ECG detection on the skin with the hydrogel damper and a commercial 3M electrode. (**F**) Frequency ranges of ECG, tapping, breathing, and walking signals. (**G**) ECG signals measured with a commercially available 3M electrode, after bandpass filtering of 0.5 to 40 Hz and (top) additional bandstop filtering and (bottom) using the hydrogel damper under mechanical noise application: tapping, breathing, and walking. (**H**) Another potential application in EEG detection under 10-Hz noise applied with an actuator. (**I**) Typical frequency ranges of EEG and 10-Hz actuation signals. (**J**) Wavelet analysis of EEG signals with (middle) a 3M electrode, (bottom) a commercial electrode with a bandstop centered at 10 Hz, and (top) the hydrogel damper during eye closing and opening. The alpha wave region (8 to ~12 Hz) is targeted under external mechanical noise (10 Hz).

create various scales of friction (*29*). A Morelet wavelet transforms analysis shows that using the control sensors with PDMS and bandpass filtering with 80 to 200 Hz, the vocal signals and swallowing motion could barely be identified (Fig. 4C, fig. S15, and movie S3). By contrast, the spectrogram of the sensor with the hydrogel damper shows a relatively clear separation of acoustic signals from the swallowing motion signal; even at 40°C with the integrated heater, entire noise signals due to motion disappear (fig. S16). The reference, even with the bandpass filtering at 80 to 200 Hz, shows a broad frequency range with the lowest signal-to-noise ratio (SNR), which means that the target signal acquisition is inaccurate, making it hard to discriminate signal from noise (Fig. 4D). With the hydrogel damper, the peak frequency ranges become narrow, and the SNR increases with the temperature (fig. S17). Another example of acquisition, heart rate signals (0.3 to 4 Hz) on the wrist under the lifting move or tapping (<0.4 Hz), supports that the selective mechanical signal target can be exploited regardless of the mechanical noises (fig. S18).

Because the hydrogel damper can be used as a conductive electrode as well as a damping material, we next explored whether it can be used to obtain electrophysiological signals (ECG and EEG) (Fig. 1H and fig. S13). The hydrogel can be expected to transmit the electrophysiology while damping the external mechanical noises. With the lower impedance of the hydrogel (fig. S13), one demonstration involves ECG signal detection (0.05 to 150 Hz range) measurement by attaching each electrode to the chest of a volunteer (Fig. 4E) while the electrode is tapped (7 to 8 Hz) and the participant is breathing and walking (1 to 2 Hz) (Fig. 4F). When the representative signals before and after mechanical noise application were analyzed, the mechanical noise obscured the ECG waveforms, whereas the ECG signal was detected in the hydrogel case regardless of mechanical noise (Fig. 4G). Even bandpass filtering of 0.5 to 40 Hz and additional arbitrary bandstop filtering were ineffective in each case because the noise frequency was within the frequency ranges of the target signals. By contrast, the hydrogel damper results show representative signals that were stable and clear regardless of external mechanical noise (fig. S19). During continuous biophysiology detection over a full day, the mechanical noise-damping capability was not degraded (fig. S20).

We also measured EEG alpha wave signals (8 to 12 Hz) when the eyes are closing by attaching the electrodes to a volunteer's forehead, together with an actuator that generates 10 Hz mechanical noise (Fig. 4, H and I). The wavelet spectrogram shows that both the hydrogel damper and commercial electrodes detect electrical signals at ~9 to 12 Hz when the volunteer closes their eyes (Fig. 4J). When the eyes are open, in which case no signals should appear at 9 to 12 Hz, continuous 10-Hz noise was detected in the commercial electrode cases, and even bandstop filtering of 10 Hz was inefficient because it distorted the signals. However, the hydrogel damper damps the 10-Hz noise selectively, and intermittent signals at 9 to 12 Hz are detected by the hydrogel damper during natural eye closing, indicating that stable electrical signal acquisition is achieved regardless of the noise (fig. S21).

Selective frequency damping with the viscoelastic material minimizes mechanical noise and enables the detection of biophysiological signals with a high SNR under noisy conditions. Rather than signal processing after the interruption by the mechanical noises, selective frequency damping by the material itself would be more effective to acquire clear signals. The strategy for the engineering of relaxation time on demand becomes essential under the various environmental conditions and needs to be further improved in the future work—as well as the temperature controls, which may require additional form factors in whole devices, and the skin can suffer from the temperature controls. In this way, we propose that the real-time application of soft bioelectronics that does not require a signal-processing step can be accelerated with viscoelastic soft materials compared with that of rigid wearable electronics.

REFERENCES AND NOTES

1. D.-H. Kim *et al*., *Science* **333**, 838–843 (2011).
2. S. Lee *et al*., *Science* **370**, 966–970 (2020).
3. J. Lee *et al*., *Nat. Electron.* **4**, 291–301 (2021).
4. T.-i. Kim *et al*., *Science* **340**, 211–216 (2013).
5. J. Deng *et al*., *Nat. Mater.* **20**, 229–236 (2021).
6. C. S. Boland *et al*., *Science* **354**, 1257–1260 (2016).
7. E. Song, J. Li, S. M. Won, W. Bai, J. A. Rogers, *Nat. Mater.* **19**, 590–603 (2020).
8. S. P. Lacour, G. Courtine, J. Guck, *Nat. Rev. Mater.* **1**, 16063 (2016).
9. M. Baumgartner *et al*., *Nat. Mater.* **19**, 1102–1109 (2020).
10. O. A. Araromi *et al*., *Nature* **587**, 219–224 (2020).
11. A. Pena-Francesch, H. Jung, M. C. Demirel, M. Sitti, *Nat. Mater.* **19**, 1230–1235 (2020).
12. I. You *et al*., *Science* **370**, 961–965 (2020).
13. B. C.-K. Tee *et al*., *Science* **350**, 313–316 (2015).
14. K. Lee *et al*., *Nat. Biomed. Eng.* **4**, 148–158 (2020).
15. C. J. De Luca, L. D. Gilmore, M. Kuznetsov, S. H. Roy, *J. Biomech.* **43**, 1573–1579 (2010).
16. F. G. Barth, *A Spider's World: Senses and Behavior* (Springer, 2002).
17. S. L. Young *et al*., *Acta Biomater.* **10**, 4832–4842 (2014).
18. J. F. Vincent, *Compos., Part A Appl. Sci. Manuf.* **33**, 1311–1315 (2002).
19. L. Xu *et al*., *Sci. Adv.* **5**, eaau3442 (2019).
20. K. Liu *et al*., *J. Am. Chem. Soc.* **143**, 1162–1170 (2021).
21. E. K. Antonsson, R. W. Mann, *J. Biomech.* **18**, 39–47 (1985).
22. K. L. Venkatachalam, J. E. Herbrandson, S. J. Asirvatham, *Circ. Arrhythm. Electrophysiol.* **4**, 965–973 (2011).
23. S. Brage, N. Brage, P. W. Franks, U. Ekelund, N. J. Wareham, *Eur. J. Clin. Nutr.* **59**, 561–570 (2005).
24. T. McLeish, *Adv. Phys.* **51**, 1379–1527 (2002).
25. M. Tang *et al*., *ACS Omega* **2**, 2214–2223 (2017).
26. J. A. Plaizier-Vercammen, E. Lecluse, P. Boute, R. E. De Neve, *Dent. Mater.* **5**, 301–305 (1989).
27. D. Kang *et al*., *Nature* **516**, 222–226 (2014).
28. B. Park *et al*., *Adv. Mater.* **28**, 8130–8137 (2016).
29. T. Cristiani *et al*., *Tribol. Lett.* **66**, 149 (2018).
30. A. P. Unwin *et al*., *Sci. Rep.* **8**, 2454 (2018).

ACKNOWLEDGMENTS

The authors thank S. J. Kwon (SKKU) for helpful discussion on the theoretical modeling; D. S. Hwang (Postech) for the chitosan hydrogel; D. Kim (SKKU) for the high-speed camera; and H.-J. Chung (University of Alberta), H. Lee (KAIST), B. Jin, and S. Jo for helpful discussion on the hydrogel. **Funding:** This work was supported by National Research Foundation of Korea (NRF) grants funded by the Korean government (MSIT) (NRF-2019R1I1A2A01061966, NRF-2020M3C1B8016137, and NRF-2019M3C7A1032076) and by the Technology Innovation Program (20013794, Center for Composite Materials and Concurrent Design) funded by the Ministry of Trade, Industry & Energy (MOTIE, Korea). B.P. was partially supported by Korea Institute for Advancement of Technology (KIAT) grant funded by the Korea Government (MOTIE) [P0017305, Human Resource Development Program for Industrial Innovation (Global)]. **Ethics statement:** All human subject experiments conducted with the volunteers were preapproved by the human subject review board of Sungkyunkwan University (ISKKU 2019-06-015). **Author contributions:** B.P. and T.-i.K. designed the experiments and led this work. B.P. and S.P. synthesized the hydrogel damper. B.P., J.O., and S.P. investigated the mechanical properties of the hydrogel damper. B.P., W.J., C.J., S.C., and Y.J.J. investigated the properties of gelatin and chitosan. B.P. and J.H.S. implemented the detection of biophysiological signals with the hydrogel damper. All authors discussed and shared the results and ideas. B.P. and T.-i.K. wrote the paper. **Competing interests:** T.-i.K, B.P., and S.P. are inventers on a patent application related to this work (KR 10-2020-0061065, 12 May 2021). The authors declare no other competing interests. **Data and materials availability:** All data are available in the main text or the supplementary materials.

SUPPLEMENTARY MATERIALS

science.org/doi/10.1126/science.abj9912
Materials and Methods
Supplementary Text
Figs. S1 to S21
Table S1 and S2
References (*31*–*43*)
Movies S1 to S4

Submitted 16 June 2021; accepted 31 March 2022
10.1126/science.abj9912

Science

Cuticular pad–inspired selective frequency damper for nearly dynamic noise–free bioelectronics

Byeonghak ParkJoo Hwan ShinJehyung OkSubin ParkWoojin JungChanho JeongSeunghwan ChoyYoung Jin JoTae-il Kim

Science, 376 (6593), • DOI: 10.1126/science.abj9912

Bioinspired frequency dampening

Physical activity can interfere with the measurement of physiological signals and often requires band-pass filtering to remove the artifacts. Park *et al*. draw inspiration from the viscoelastic properties of the cuticular pad of spiders that can separate target vibration signals from mechanical noise. They developed a gelatin/chitosan hydrogel damper that will absorb frequencies below 30 hertz, whereas higher frequencies transmit due to the temporary disruption of the weak internetwork bonds in the hydrogel. The authors show that the hydrogel can be used to detect electrophysiological signals such as electroencephalograms and electrocardiograms without interference caused by the patient's walking or breathing. —MSL